

Fall 9-8-2020

## Precision Measurement of the Beam-Normal Single-Spin Asymmetry in Forward-Angle Elastic Electron-Proton Scattering

Qweak Collaboration  
*William & Mary*

David Armstrong  
dsarms@wm.edu

Wouter Deconinck  
*William & Mary*

K. Bartlett  
*William & Mary*

J. C. Cornejo  
*William & Mary*

*See next page for additional authors*

Follow this and additional works at: <https://scholarworks.wm.edu/aspubs>



Part of the [Elementary Particles and Fields and String Theory Commons](#), and the [Nuclear Commons](#)

---

### Recommended Citation

Qweak Collaboration; Armstrong, David; Deconinck, Wouter; Bartlett, K.; Cornejo, J. C.; Carlini, R. D.; Dowd, James F.; Finn, J. M.; Gray, Valerie M.; Grimm, K.; Hoskins, J. R.; Leckey, J. P.; Lee, Jeong Han; Magee, Joshua A.; and Owen, Victoria F., Precision Measurement of the Beam-Normal Single-Spin Asymmetry in Forward-Angle Elastic Electron-Proton Scattering (2020). *Physical Review Letters*, 125(11), 112502. <https://doi.org/10.1103/PhysRevLett.125.112502>

This Article is brought to you for free and open access by the Arts and Sciences at W&M ScholarWorks. It has been accepted for inclusion in Arts & Sciences Articles by an authorized administrator of W&M ScholarWorks. For more information, please contact [scholarworks@wm.edu](mailto:scholarworks@wm.edu).

---

**Authors**

Qweak Collaboration, David Armstrong, Wouter Deconinck, K. Bartlett, J. C. Cornejo, R. D. Carlini, James F. Dowd, J. M. Finn, Valerie M. Gray, K. Grimm, J. R. Hoskins, J. P. Leckey, Jeong Han Lee, Joshua A. Magee, and Victoria F. Owen

## Precision Measurement of the Beam-Normal Single-Spin Asymmetry in Forward-Angle Elastic Electron-Proton Scattering

D. Androić,<sup>1</sup> D. S. Armstrong,<sup>2,†</sup> A. Asaturyan,<sup>3</sup> K. Bartlett,<sup>2</sup> J. Beaufait,<sup>4</sup> R. S. Beminiwatha,<sup>5,6</sup> J. Benesch,<sup>4</sup> F. Benmokhtar,<sup>7</sup> J. Birchall,<sup>8</sup> R. D. Carlini,<sup>4,2</sup> J. C. Cornejo,<sup>2</sup> S. Covrig Dusa,<sup>4</sup> M. M. Dalton,<sup>9,4</sup> C. A. Davis,<sup>10</sup> W. Deconinck,<sup>2</sup> J. F. Dowd,<sup>2</sup> J. A. Dunne,<sup>11</sup> D. Dutta,<sup>11</sup> W. S. Duvall,<sup>12</sup> M. Elaasar,<sup>13</sup> W. R. Falk,<sup>8,\*</sup> J. M. Finn,<sup>2,\*</sup> T. Forest,<sup>14,6</sup> C. Gal,<sup>9</sup> D. Gaskell,<sup>4</sup> M. T. W. Gericke,<sup>8</sup> J. Grames,<sup>4</sup> V. M. Gray,<sup>2</sup> K. Grimm,<sup>6,2</sup> F. Guo,<sup>15</sup> J. R. Hoskins,<sup>2</sup> D. Jones,<sup>9</sup> M. K. Jones,<sup>4</sup> R. T. Jones,<sup>16</sup> M. Kargiantoulakis,<sup>9</sup> P. M. King,<sup>5</sup> E. Korkmaz,<sup>17</sup> S. Kowalski,<sup>15</sup> J. Leacock,<sup>12</sup> J. P. Leckey,<sup>2</sup> A. R. Lee,<sup>12</sup> J. H. Lee,<sup>5,2</sup> L. Lee,<sup>10,8</sup> S. MacEwan,<sup>8</sup> D. Mack,<sup>4</sup> J. A. Magee,<sup>2</sup> R. Mahurin,<sup>8</sup> J. Mammei,<sup>8,12</sup> J. W. Martin,<sup>18</sup> M. J. McHugh,<sup>19</sup> D. Meekins,<sup>4</sup> J. Mei,<sup>4</sup> K. E. Mesick,<sup>19,20</sup> R. Michaels,<sup>4</sup> A. Micherdzinska,<sup>19</sup> A. Mkrtchyan,<sup>3</sup> H. Mkrtchyan,<sup>3</sup> N. Morgan,<sup>12</sup> A. Narayan,<sup>11</sup> L. Z. Ndukum,<sup>11</sup> V. Nelyubin,<sup>9</sup> Nuruzzaman,<sup>21,11</sup> W. T. H. van Oers,<sup>10,8</sup> V. F. Owen,<sup>2</sup> S. A. Page,<sup>8</sup> J. Pan,<sup>8</sup> K. D. Paschke,<sup>9</sup> S. K. Phillips,<sup>22</sup> M. L. Pitt,<sup>12</sup> R. W. Radloff,<sup>5</sup> J. F. Rajotte,<sup>15</sup> W. D. Ramsay,<sup>10,8</sup> J. Roche,<sup>5</sup> B. Sawatzky,<sup>4</sup> T. Seva,<sup>1</sup> M. H. Shabestari,<sup>11</sup> R. Silwal,<sup>9</sup> N. Simicevic,<sup>6</sup> G. R. Smith,<sup>4</sup> P. Solvignon,<sup>4,\*</sup> D. T. Spayde,<sup>23</sup> A. Subedi,<sup>11</sup> R. Subedi,<sup>19</sup> R. Suleiman,<sup>4</sup> V. Tadevosyan,<sup>3</sup> W. A. Tobias,<sup>9</sup> V. Tvaskis,<sup>18</sup> B. Waidyawansa,<sup>5,6</sup> P. Wang,<sup>8</sup> S. P. Wells,<sup>6</sup> S. A. Wood,<sup>4</sup> S. Yang,<sup>2</sup> P. Zang,<sup>24</sup> and S. Zhamkochyan<sup>3</sup>

(Q<sub>weak</sub> Collaboration)

<sup>1</sup>University of Zagreb, Zagreb, HR 10002, Croatia

<sup>2</sup>William & Mary, Williamsburg, Virginia 23185, USA

<sup>3</sup>A. I. Alikhanyan National Science Laboratory (Yerevan Physics Institute), Yerevan 0036, Armenia

<sup>4</sup>Thomas Jefferson National Accelerator Facility, Newport News, Virginia 23606, USA

<sup>5</sup>Ohio University, Athens, Ohio 45701, USA

<sup>6</sup>Louisiana Tech University, Ruston, Louisiana 71272, USA

<sup>7</sup>Duquesne University, Pittsburgh, Pennsylvania 15282, USA

<sup>8</sup>University of Manitoba, Winnipeg, Manitoba R3T2N2, Canada

<sup>9</sup>University of Virginia, Charlottesville, Virginia 22903, USA

<sup>10</sup>TRIUMF, Vancouver, British Columbia V6T2A3, Canada

<sup>11</sup>Mississippi State University, Mississippi State, Mississippi 39762, USA

<sup>12</sup>Virginia Polytechnic Institute & State University, Blacksburg, Virginia 24061, USA

<sup>13</sup>Southern University at New Orleans, New Orleans, Louisiana 70126, USA

<sup>14</sup>Idaho State University, Pocatello, Idaho 83209, USA

<sup>15</sup>Massachusetts Institute of Technology, Cambridge, Massachusetts 02139, USA

<sup>16</sup>University of Connecticut, Storrs-Mansfield, Connecticut 06269, USA

<sup>17</sup>University of Northern British Columbia, Prince George, British Columbia V2N4Z9, Canada

<sup>18</sup>University of Winnipeg, Winnipeg, Manitoba R3B2E9, Canada

<sup>19</sup>George Washington University, Washington, DC 20052, USA


<sup>20</sup>Rutgers, The State University of New Jersey, Piscataway, New Jersey 088754, USA

<sup>21</sup>Hampton University, Hampton, Virginia 23668, USA

<sup>22</sup>University of New Hampshire, Durham, New Hampshire 03824, USA

<sup>23</sup>Hendrix College, Conway, Arkansas 72032, USA

<sup>24</sup>Syracuse University, Syracuse, New York 13244, USA

 (Received 23 June 2020; revised 7 August 2020; accepted 11 August 2020; published 8 September 2020)

A beam-normal single-spin asymmetry generated in the scattering of transversely polarized electrons from unpolarized nucleons is an observable related to the imaginary part of the two-photon exchange process. We report a 2% precision measurement of the beam-normal single-spin asymmetry in elastic electron-proton scattering with a mean scattering angle of  $\theta_{\text{lab}} = 7.9^\circ$  and a mean energy of 1.149 GeV. The asymmetry result is  $B_n = -5.194 \pm 0.067(\text{stat}) \pm 0.082(\text{syst})$  ppm. This is the most precise measurement of this quantity available to date and therefore provides a stringent test of two-photon exchange models at far-forward scattering angles ( $\theta_{\text{lab}} \rightarrow 0$ ) where they should be most reliable.

DOI: 10.1103/PhysRevLett.125.112502

The high intensities of electron beams at facilities like Jefferson Lab and MAMI make them ideal for studying the charge and magnetization distributions inside nuclear matter in the single-photon exchange (Born) approximation. However, high precision measurements can be affected by two-photon exchange (TPE) [1]. Depending on the observable, either the real or imaginary part of the TPE amplitude can play a role.

There has been significant effort to study the real part of the TPE amplitude because it affects cross sections [1]. However, the uncertainties in the theoretical calculations are large, and constraints on models remain weak even after a decade-long program of targeted measurements [1]. An alternative approach is to study observables proportional to the imaginary part of the TPE amplitude such as the beam-normal single-spin asymmetry ( $A_y$  [2], or  $B_n$ ).

$B_n$  is a parity- and  $CP$ -conserving asymmetry typically at the few parts-per-million (ppm) level for forward angles and GeV-scale incident energies in  $\vec{e}p$  elastic scattering. Required by time-reversal invariance to vanish in the one-photon exchange approximation, a nonzero  $B_n$  can only arise with the exchange of two or more photons between the scattered electron and the target nucleon [3]. Experimentally,  $B_n$  manifests itself as the amplitude of an azimuthal variation of the asymmetry when the beam is polarized transverse to its incident momentum.

Theoretically, two complementary approaches have been pursued. One [4,5] is expected to be valid at all angles, but should work best at lower energies because it only includes the  $\pi N$  intermediate state as well as the (smaller) elastic proton contribution. The other approach [1,3,6–11] is expected to work at all energies because it includes contributions from multiparticle intermediate states (e.g.,  $\pi\pi N, \eta N, K\Lambda, \dots$ ), but works best at forward angles because it uses the optical theorem to relate the measured total photoproduction cross section to the imaginary part of the TPE forward scattering amplitude  $\mathcal{I}m(\text{TPE})$ .

Hard TPE was generally treated as causing small (percent-level) corrections to the unpolarized scattering cross section that are independent of hadronic structure [12,13]. However, in 2000, a striking disagreement in the proton's elastic electromagnetic form-factor ratio ( $G_E^p/G_M^p$ ) was observed when comparing Rosenbluth ( $L/T$ ) separation [14] and polarization transfer [15] results at  $Q^2 \geq 2$  (GeV/c)<sup>2</sup>. This discrepancy (known as the proton form-factor puzzle) could be explained [16] by a correction involving the real part of the TPE amplitude that modifies the Rosenbluth cross section, but largely cancels in the polarization-transfer ratios. A recent summary can be found in [1].

The real part of the TPE amplitude  $\mathcal{R}e(\text{TPE})$  can be determined from the ratio of  $e^\pm p$  cross sections (see VEPP-3 [17], OLYMPUS [18], CLAS [19]). In principle,  $\mathcal{R}e(\text{TPE})$  can also be determined from the imaginary part via dispersion relations. In practice, this is difficult since a

broad range of kinematics is needed and there is a paucity of  $B_n$  results. Nevertheless, the effects of TPE on the proton radius puzzle (see [20] for the most recent results and a summary) have been explored theoretically [7] using an unsubtracted fixed- $t$  dispersion relation to do just that, predicting that TPE effects are at the level of the present uncertainties ( $\approx 1\%$ ) in the proton radius determinations from  $ep$  scattering data. Future experiments (MUSE [21,22]) aim to improve this precision and further explore TPE effects by comparing  $e^\pm p$  and  $\mu^\pm p$  scattering. This underscores the importance of providing  $B_n$  data to test the predictions of  $\mathcal{I}m(\text{TPE})$ .

The kinematics of this experiment are at a far-forward electron scattering angle ( $7.9^\circ$ ), where the optical model approach should work well, and with a small four-momentum transfer  $Q^2 = -t = 0.0248$  (GeV/c)<sup>2</sup> and an intermediate energy ( $E_{\text{lab}} = 1.149$  GeV,  $E_{\text{cm}} = 1.74$  GeV), where up to five pion intermediate states can contribute. The asymmetry is generated by the interference of one- and two-photon exchange processes and has the form [23]

$$B_n = \frac{\sigma^\uparrow - \sigma^\downarrow}{\sigma^\uparrow + \sigma^\downarrow} = \frac{2\mathcal{I}m(\mathcal{M}_{\gamma\gamma}\mathcal{M}_\gamma^*)}{|\mathcal{M}_\gamma|^2}, \quad (1)$$

where  $\sigma^\uparrow(\sigma^\downarrow)$  denotes the scattering cross section for electrons with spin parallel (antiparallel) to a vector  $\hat{n}$  normal to the scattering plane, where  $\hat{n} = (\vec{k} \times \vec{k}')/(|\vec{k} \times \vec{k}'|)$ , with  $\vec{k}(\vec{k}')$  being the momentum of the incoming (outgoing) electron.  $\mathcal{M}_\gamma$  and  $\mathcal{M}_{\gamma\gamma}$  are the amplitudes for one- and two-photon exchange. For transversely polarized electrons scattering from unpolarized nucleons, the detected asymmetry then depends on the azimuthal scattering angle  $\phi$  via  $A_{\text{exp}}(\phi) \approx B_n \vec{P} \cdot \hat{n}$ , where  $\vec{P}$  is the electron polarization vector.

Companion measurements of  $B_n$  are necessary in most parity-violating electron scattering experiments in order to account for the effects of residual transverse polarization in the nominally longitudinally polarized beam. Previous measurements of  $B_n$  at far-forward angles ( $6.0^\circ < \theta_{\text{lab}} < 9.7^\circ$ ) were obtained by the G0 [24] and HAPPEX [25] collaborations with  $E_{\text{lab}}$  near 3 GeV. Somewhat larger-angle results have been obtained by PVA4 [26,27] for  $(\theta_{\text{lab}}, E_{\text{lab}}) = (\approx 34^\circ, 0.3\text{--}1.5$  GeV), and by SAMPLE [28] at  $(\approx 55^\circ, 0.2$  GeV). Backward angle experiments were performed at  $(180^\circ, 0.36$  and  $0.69$  GeV) by G0 [29] and at  $(145^\circ, 0.32$  and  $0.42$  GeV) by PVA4 [30]. Some of these experiments also included results on deuterium [29,30], as well as heavier nuclei [25].

The  $(7.9^\circ, 1.149$  GeV) elastic  $\vec{e}p$   $B_n$  measurement reported here was part of a series of companion measurements performed by the  $Q_{\text{weak}}$  collaboration to constrain systematic uncertainties in the first determination of the weak charge of the proton [31,32]. The general performance of the experimental apparatus is described

in Ref. [33]. Details relevant to the extraction of  $B_n$  are presented here.

A total of 54 h of  $B_n$  data were collected in three measurement periods and with two different orientations of transverse polarization. Polarized electrons were generated by photoemission from a strained GaAs cathode at the injector of the Thomas Jefferson National Accelerator Facility. Two Wien filters [34] were used to rotate the electron spin in the transverse plane to horizontal (spin pointing to beam-right at the target) or vertical (spin pointing up). The transversely polarized, 150–180  $\mu\text{A}$  electron beam was then accelerated to 1.16 GeV before reaching the  $Q_{\text{weak}}$  apparatus in experimental Hall C. There it scattered from unpolarized liquid hydrogen encased in a 34.4-cm-long aluminum-alloy cell with thin (0.1-mm-thick) windows where the beam entered and exited. Longitudinal polarization measurements (bracketing the transverse running) using Møller and Compton polarimeters [35–37] upstream of the target yielded an average statistics-weighted beam polarization  $\langle P \rangle = (88.72 \pm 0.70)\%$ . During the transverse running, the polarization was verified to be  $>99.97\%$  transverse via null measurements with the Møller polarimeter, which is only sensitive to longitudinal beam polarization.

A set of collimators located downstream of the target selected electrons with lab scattering angles of  $5.8^\circ$ – $11.6^\circ$ . A toroidal magnet then focused elastic electrons onto a set of eight Cherenkov detectors placed symmetrically around the beam axis, 12.2 m downstream of the target. The azimuthal coverage of the detector array was 49% of  $2\pi$ .

The spin direction of the electrons was selected from one of two pseudorandomly chosen quartet patterns ( $\uparrow\downarrow\downarrow\uparrow$  or  $\downarrow\uparrow\uparrow\downarrow$ ) generated at 240 Hz. Here  $\uparrow$  represents the standard spin orientation (spin up or to beam right) and  $\downarrow$  represents a  $180^\circ$  rotation in the corresponding plane. The signals from the Cherenkov detectors were integrated for each  $\uparrow$  and  $\downarrow$  spin state (at 960 Hz). The detector asymmetries were calculated for each quartet using  $A_{\text{raw}} = [(Y_\uparrow - Y_\downarrow)/(Y_\uparrow + Y_\downarrow)]$ , where  $Y_{\uparrow(\downarrow)}$  is the charge-normalized detector yield in the  $\uparrow$  or  $\downarrow$  spin state. The systematic uncertainty due to the beam charge normalization was negligible here [31]. False asymmetries from spin-correlated beam position, angle, and energy changes were largely canceled by the periodic insertion of a half wave plate located in the injector. Further suppression of false asymmetries was achieved by using  $A_{\text{msr}} = A_{\text{raw}} - \sum_{j=1}^5 (\partial A/\partial \chi_j) \Delta \chi_j$ , where  $\Delta \chi_j$  are the helicity-correlated differences in beam position (vertical and horizontal), beam angle (vertical and horizontal), and beam energy over the helicity quartet, and the slopes  $\partial A/\partial \chi_j$  were determined using multivariable linear regression [38]. False asymmetries caused by secondary events scattered from beam line elements were negligible ( $<0.005$  ppm) [31].

The measured asymmetries  $A_{\text{msr}}^i$  in detector  $i$ , for both orientations of the transverse beam polarization, were fit to

$$A_{\text{msr}}^i(\phi_i) = R_l R_{\text{av}} A_{\text{exp}} \sin(\phi_s - \phi_i + \phi_{\text{off}}) + C, \quad (2)$$

to extract the experimental asymmetry  $A_{\text{exp}}$ . Here  $\phi_s$  is the azimuthal angle of  $\vec{P}$ , and  $\phi_i$  is the azimuthal angle of the  $i$ th detector in the plane normal to the beam axis. The factor  $R_{\text{av}} = 0.9938 \pm 0.0006$  accounts for the averaging of the asymmetry over the effective azimuthal acceptance ( $\approx 22^\circ$ ) of a Cherenkov detector and  $R_l = 1.007 \pm 0.005$  corrects for the measured nonlinearity in the detector electronics. A floating offset in phase  $\phi_{\text{off}}$  was included to account for any detector offsets in the azimuthal plane, and a floating constant  $C$  was included to represent any monopole asymmetries, such as due to parity-violating asymmetry generated by any residual longitudinal beam polarization. The fitted values for  $\phi_{\text{off}}$  and  $C$  were consistent with zero, and the value of  $A_{\text{exp}}$  extracted was insensitive to the inclusion of these extra fit parameters.

The fits to Eq. (2) for the three datasets are shown in Fig. 1. Since the kinematics were similar and the results consistent, the error-weighted average of the three measurements  $A_{\text{exp}} = -4.801 \pm 0.056(\text{stat}) \pm 0.039(\text{syst})$  ppm was used as the experimental asymmetry from the full measurement. The systematic error accounts for the uncertainties in  $R_l$ ,  $R_{\text{av}}$  and the linear regression.

The experimental asymmetry  $A_{\text{exp}}$  was then corrected for four backgrounds. The largest background was  $f_1 = 3.3 \pm 0.2\%$ , a dilution from elastic and quasielastic electrons scattering from the aluminum-alloy beam entrance and exit windows of the target. Dedicated measurements using an aluminum-alloy target, similar to but thicker than the windows used in the target cell, were used to determine

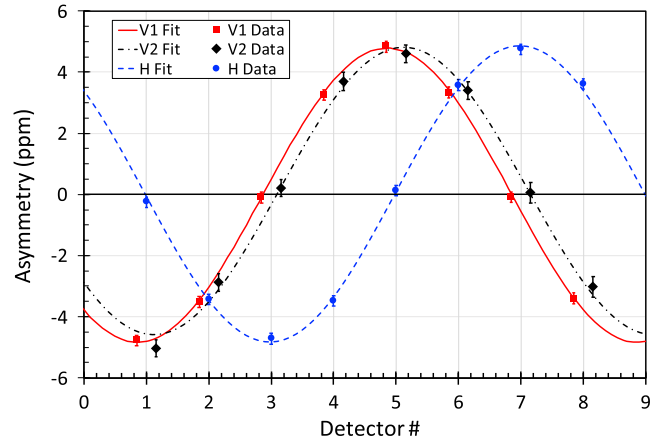


FIG. 1. Extraction of the experimental asymmetry  $A_{\text{exp}}$  from the measured asymmetries  $A_{\text{msr}}^i$  for the horizontal (H) and the two vertical datasets (V1 and V2). The phases of the vertical datasets were offset  $-7^\circ$  (V1) and  $+7^\circ$  (V2) in the figure for clarity. The detector number corresponds to the azimuthal location of the detectors, starting from beam left (detector 1), where  $\phi_i = 0^\circ$ , and increasing clockwise every  $45^\circ$ . Uncertainties shown are statistical only. The reduced  $\chi^2$  (5 degrees of freedom) in the fits are 0.15 (V1), 1.07 (V2), and 0.81 (H).



TABLE I. Summary of experimental uncertainties.

Uncertainty source	$\Delta B_n/B_n$ (%)
Statistics	1.29
Systematics	
$P$ : beam polarization	0.807
$R_{\text{tot}}$ : kinematics and acceptance	0.428
$R_f$ : electronic nonlinearity	0.540
Linear regression	0.656
$R_{\text{av}}$ : acceptance averaging	0.067
$A_1$ : aluminum background asymmetry	0.408
$f_1$ : aluminum dilution	0.172
$A_2$ : inelastic background asymmetry	0.024
$f_2$ : inelastic dilution	0.030
$A_3$ : beam line neutral asymmetry	0.004
$f_3$ : beam line neutral dilution	0.064
$A_4$ : other neutral background asymmetry	0.201
$f_4$ : other neutral background dilution	0.213
$A_{\text{bias}}$	0.789
Systematics subtotal	1.57
Total uncertainty	2.03

the aluminum asymmetry  $A_1$  [38]. Another background correction was applied for  $f_2 = 0.018 \pm 0.004\%$ , a dilution due to inelastic electrons. The inelastic asymmetry  $A_2$  [38] was determined using dedicated measurements with the toroidal magnet configured to focus inelastic electrons onto the detectors. Additionally, neutral backgrounds in the acceptance generated by sources in the beam line ( $f_3 = 0.19 \pm 0.06\%$  dilution) and other sources ( $f_4 < 0.3\%$  dilution) were studied. These neutral backgrounds constituted negligible corrections to the experiment's final azimuthal asymmetry. Therefore, no correction was applied ( $A_3 \approx A_4 \approx 0$ ). However, their dilutions were taken into consideration.

A unique potential background asymmetry not yet observed in a  $B_n$  measurement is a parity-violating beam-transverse single-spin asymmetry ( $A_x$ ), generated by the interference between one-photon exchange and the  $Z^0$  exchange processes. At our kinematics,  $A_x$  is estimated to be on the order of  $10^{-11}$  [39], too small to be observed in this experiment.

The various corrections were applied to the experimental asymmetry  $A_{\text{exp}}$  to extract  $B_n$  following

$$B_n = R_{\text{tot}} \left[ \frac{A_{\text{exp}}/P - \sum_{i=1}^4 f_i A_i}{1 - \sum_{i=1}^4 f_i} \right] + A_{\text{bias}}. \quad (3)$$

Here  $A_i$  is the background asymmetry generated by the  $i$ th background (aluminum windows, inelastics, beam line neutrals, and other neutrals, respectively) with dilution  $f_i$ . The factor  $R_{\text{tot}} = 1.0041 \pm 0.0046$  accounts for electron energy loss and depolarization from electromagnetic radiation, nonuniform  $Q^2$  distribution across the detectors, light-collection variation across the detectors, and the

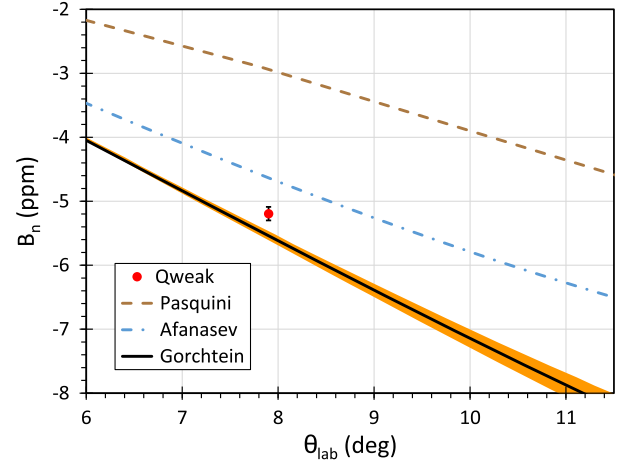


FIG. 2. Comparison of this measurement (red circle) to calculations at  $E_{\text{lab}} = 1.149$  GeV by Pasquini and Vanderhaeghen [4], Afanasev and Merenkov [10], and Gorchtein [6] over the  $Q_{\text{weak}}$  acceptance. The orange band about the latter calculation indicates the model uncertainty.

uncertainty in the acceptance-averaged  $\langle Q^2 \rangle = 0.0248 \pm 0.0001$  GeV<sup>2</sup>.  $A_{\text{bias}} = 0.125 \pm 0.041$  ppm is a false asymmetry that arose due to the analyzing power of the scattered electrons that can rescatter in the lead preradiators installed upstream of each main detector. This effect is described in detail elsewhere [31]; it was larger in magnitude in the present case because, for a transversely polarized beam, it does not largely cancel due to the symmetry of the apparatus. With the above corrections, we obtain a value of  $B_n = -5.194 \pm 0.067$  (stat)  $\pm 0.082$  (syst) ppm for elastic electron-proton scattering at a vertex scattering angle of  $\langle \theta \rangle = 7.9^\circ$  and vertex energy  $\langle E \rangle = 1.149$  GeV. The contributions from different error sources are summarized in Table I and discussed in more detail in Ref. [38].

Figure 2 compares our measurement to three model calculations: Pasquini and Vanderhaeghen [4,5], Afanasev and Merenkov [10,11], and Gorchtein [3,6–9]. The latter model [3,6–9] is in closest agreement with this measurement (within 0.3 ppm, or just 7%), but still  $2.7\sigma$  away, given the small  $Q_{\text{weak}}$  uncertainty. The other prediction that also uses the optical theorem [10,11] is only slightly further away. The Pasquini and Vanderhaeghen model significantly underpredicts the magnitude of  $B_n$ . The latter calculation uses unitarity to model the doubly virtual Compton scattering (VVCS) tensor in the resonance regime in terms of electroabsorption amplitudes, whereas both Afanasev and Merenkov as well as Gorchtein use the optical theorem to relate the forward VVCS tensor to the total photoabsorption cross section. Although the three calculations predict similar angular behavior for the asymmetry in our acceptance, their magnitudes vary widely.

Generally, the models agree that the dominant contribution to the asymmetry comes from the inelastic intermediate states of the nucleon in TPE. The contribution from the

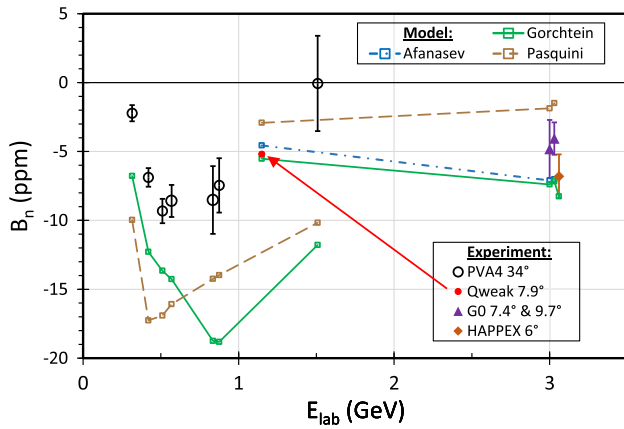


FIG. 3. Beam energy dependence of all forward-angle ( $\theta_{\text{lab}} \leq 34^\circ$ ) elastic  $\bar{e}p$   $B_n$  data compared to calculations at each experiment's kinematics. The far-forward-angle data (solid symbols,  $\theta_{\text{lab}} < 10^\circ$ ) are from this experiment (red circle, uncertainty smaller than the symbol), G0 [24] (purple triangles), and HAPPEX [25] (orange diamond). Less-forward-angle data  $\theta_{\text{lab}} \approx 34^\circ$  are denoted with open circles from PVA4 [26,27] (black). The predictions (open squares) from each theoretical group (Pasquini and Vanderhaeghen [4,5], Afanasev and Merenkov [10,11], and Gorchtein [3,6–9]) are connected by straight-line segments for the far-forward and the forward-angle calculations to help guide the eye.

elastic state is insignificant. However, both the Afanasev and Merenkov model and the Gorchtein model consider all inelastic intermediate states with multipion excitations, whereas the Pasquini and Vanderhaeghen model only considers inelastic states with single-pion excitations. This likely causes the largest difference between the two types of calculations [5,9,11].

The calculations from the three theoretical groups discussed here differ at different kinematics, making a global comparison to other experiments difficult. For example, the Gorchtein model includes corrections to account for the off-forward  $34^\circ$  data of [27], which are not used to predict the far-forward  $7.9^\circ$  kinematics of this experiment. However, it is still instructive to compare the existing forward-angle  $B_n$  data to the kinematics-specific predictions from each theoretical group. Such a comparison is shown as a function of  $E_{\text{lab}}$  in Fig. 3 for  $\theta_{\text{lab}} \leq 34^\circ$  data. This figure shows that all the models have significant disagreements with the less-forward-angle ( $\theta_{\text{lab}} > 10^\circ$ ) data. The far-forward data are in a better position to be described theoretically using the optical theorem and those calculations do show reasonable agreement. The  $Q_{\text{weak}}$  result provides, by far, the most precise test of models to date in the kinematic region where they are expected to be most accurate.

The beam-normal single-spin asymmetry is a unique tool to test dispersion relations used in calculating TPE corrections to  $ep$  scattering cross sections. In light of improving these TPE corrections in  $ep$  and  $\mu p$  scattering

observables, precision measurements of  $B_n$  are extremely useful for validating TPE models. The precise  $Q_{\text{weak}}$  datum reported here, in particular, provides a stringent test of the TPE models at far-forward angles and moderate energy.

We thank the staff of Jefferson Lab, TRIUMF, and MIT Bates, as well as our undergraduate students, for their vital support during this challenging experiment. We also thank B. Pasquini, A. Afanasev, M. Gorchtein, M. Vanderhaeghen, O. Tomalak, P. Blunden, and W. Melnitchouk for useful discussions. This work was supported by the U.S. Department of Energy (DOE), Office of Science, Office of Nuclear Physics DOE Contract No. DEAC05-06OR23177, under which Jefferson Science Associates, LLC operates Jefferson Lab. Construction and operating funding for the experiment was provided through the DOE, the Natural Sciences and Engineering Research Council of Canada (NSERC), and the National Science Foundation (NSF) with university matching contributions from William & Mary, Virginia Tech, George Washington University, and Louisiana Tech University.

\*Deceased

†Corresponding author.

armd@jlab.org

- [1] A. Afanasev, P. G. Blunden, D. Hasell, and B. A. Raue, *Prog. Part. Nucl. Phys.* **95**, 245 (2017).
- [2] *Polarization Phenomena in Nuclear Reactions, Proc. Third Int. Symposium, Madison, Wisconsin*, edited by H. Barschall and W. Haeberli (University of Wisconsin Press, Madison, 1971).
- [3] M. Gorchtein, P. A. M. Guichon, and M. Vanderhaeghen, *Nucl. Phys.* **A741**, 234 (2004).
- [4] B. Pasquini and M. Vanderhaeghen, *Phys. Rev. C* **70**, 045206 (2004).
- [5] B. Pasquini (private communication).
- [6] M. Gorchtein, *Phys. Rev. C* **73**, 055201 (2006).
- [7] M. Gorchtein, *Phys. Rev. C* **90**, 052201(R) (2014).
- [8] M. Gorchtein, P. A. M. Guichon, and M. Vanderhaeghen, *Nucl. Phys.* **A741**, 234 (2004).
- [9] M. Gorchtein (private communication).
- [10] A. V. Afanasev and N. P. Merenkov, *Phys. Lett. B* **599**, 48 (2004).
- [11] A. Afanasev (private communication).
- [12] L. W. Mo and Y.-S. Tsai, *Rev. Mod. Phys.* **41**, 205 (1969).
- [13] L. C. Maximon and J. A. Tjon, *Phys. Rev. C* **62**, 054320 (2000).
- [14] M. N. Rosenbluth, *Phys. Rev.* **79**, 615 (1950).
- [15] M. K. Jones *et al.* (Jefferson Lab Hall A Collaboration), *Phys. Rev. Lett.* **84**, 1398 (2000).
- [16] P. A. M. Guichon and M. Vanderhaeghen, *Phys. Rev. Lett.* **91**, 142303 (2003).
- [17] I. A. Rachev *et al.*, *Phys. Rev. Lett.* **114**, 062005 (2015).
- [18] B. S. Henderson *et al.* (OLYMPUS Collaboration), *Phys. Rev. Lett.* **118**, 092501 (2017).
- [19] D. Adikaram *et al.* (CLAS Collaboration), *Phys. Rev. Lett.* **114**, 062003 (2015).

- [20] W. Xiong *et al.* (PRad Collaboration), *Nature (London)* **575**, 147 (2019).
- [21] R. Gilman *et al.* (MUSE Collaboration), [arXiv:1303.2160](https://arxiv.org/abs/1303.2160).
- [22] R. Gilman *et al.* (MUSE Collaboration), [arXiv:1709.09753](https://arxiv.org/abs/1709.09753).
- [23] A. De Rujula, J. Kaplan, and E. de Rafael, *Nucl. Phys.* **B35**, 365 (1971).
- [24] D. S. Armstrong *et al.* (G0 Collaboration), *Phys. Rev. Lett.* **99**, 092301 (2007).
- [25] S. Abrahamyan *et al.* (HAPPEX and PREX Collaborations), *Phys. Rev. Lett.* **109**, 192501 (2012).
- [26] F. E. Maas *et al.*, *Phys. Rev. Lett.* **94**, 082001 (2005).
- [27] B. Gou *et al.*, *Phys. Rev. Lett.* **124**, 122003 (2020).
- [28] S. P. Wells *et al.* (SAMPLE Collaboration), *Phys. Rev. C* **63**, 064001 (2001).
- [29] D. Androić *et al.* (G0 Collaboration), *Phys. Rev. Lett.* **107**, 022501 (2011).
- [30] D. Belaguer Ríos *et al.*, *Phys. Rev. Lett.* **119**, 012501 (2017).
- [31] D. Androić *et al.* ( $Q_{\text{weak}}$  Collaboration), *Nature (London)* **557**, 207 (2018).
- [32] D. Androić *et al.* ( $Q_{\text{weak}}$  Collaboration), *Phys. Rev. Lett.* **111**, 141803 (2013).
- [33] T. Allison *et al.* ( $Q_{\text{weak}}$  Collaboration), *Nucl. Instrum. Methods Phys. Res., Sect. A* **781**, 105 (2015).
- [34] J. James, P. Adderley, J. Benesch, J. Clark, J. Hansknecht *et al.*, in *Proceedings of 2011 Particle Accelerator Conference*, edited by T. Satogata and K. Brown (IEEE, New York, 2011), <http://accelconf.web.cern.ch/AccelConf/PAC2011/papers/TUP025.PDF>.
- [35] M. Hauger, A. Honegger, J. Jourdana, G. Kubona, T. Petitjeana *et al.*, *Nucl. Instrum. Methods Phys. Res., Sect. A* **462**, 382 (2001).
- [36] J. A. Magee *et al.*, *Phys. Lett. B* **766**, 339 (2017).
- [37] A. Narayan *et al.*, *Phys. Rev. X* **6**, 011013 (2016).
- [38] D. B. P. Waidyawansa, Ph.D. Thesis, Ohio University, 2013, [https://misportal.jlab.org/ul/publications/downloadFile.cfm?pub\\_id=12540](https://misportal.jlab.org/ul/publications/downloadFile.cfm?pub_id=12540).
- [39] W. Melnitchouk, P. Blunden, and P. Sachdeva (private communication).